Available online at www.sciencedirect.com
SCIENCE DIRECT®
Journal of Sound and Vibration 289 (2006) 938–951
JOURNAL OF SOUND AND VIBRATION
www.elsevier.com/locate/jsvi

Exact dynamic stiffness matrix of a three-dimensional shear beam with doubly asymmetric cross-section

B. Rafezy, W.P. Howson*

Cardiff School of Engineering, Cardiff University, Queen's Buildings, The Parade, Cardiff CF24 3AA, UK

Received 12 May 2004; received in revised form 9 December 2004; accepted 28 February 2005
Available online 14 July 2005

Abstract

The dynamic member stiffness matrix of a three-dimensional shear beam with doubly asymmetric cross-section is derived exactly from the governing, sixth-order differential equation of motion. Such a formulation accounts for the uniform distribution of mass in the member and necessitates the solution of a transcendental eigenvalue problem. This is achieved using the Wittrick–Williams algorithm, where the necessary parameters are developed using a generalised procedure. An example is given to clarify the theory, together with a small parametric study that indicates when lateral–torsional coupling may safely be ignored. The work also holds considerable potential in its application to the approximate analysis of asymmetric, multi-storey, three-dimensional frame structures.

1. Introduction

Exact dynamic member stiffness matrices (exact finite elements) that are developed from the solution of the governing differential equations have been available for beam-column members for many years. However, such a formulation leads to a transcendental eigenvalue problem that is often intractable. Early formulations [1–5] were prone to missing roots, since they did not have the benefit of the Wittrick–Williams (W–W) algorithm [6,7], which enables any required natural frequency to be converged upon to any required accuracy. Today, the algorithm has been

*Corresponding author. Tel./fax: +44 2920 874 263.
E-mail address: howson@cf.ac.uk (W.P. Howson).

0022-460X/$ - see front matter © 2005 Elsevier Ltd. All rights reserved.
doi:10.1016/j.jsv.2005.02.046

incorporated into an extensive range of elements that can be used in the analysis of two- and three-dimensional framed structures formed from members ranging from straight Bernoulli–Euler beam columns to curved Timoshenko beams [8–12].

In recent years, the coupled bending–torsional vibration of beams that have a singly asymmetric cross-section has been addressed by a small number of investigators using the exact approach. In such beams the shear centre and the centre of mass are not coincident, so the translational and torsional modes are inherently coupled as a result of this offset [13]. Hallauer and Liu [14] and Friberg [15,16] formulated the dynamic stiffness matrix of a bending–torsion coupled beam by using successive matrix operations to obtain the resulting dynamic stiffness matrix numerically, whereas Banerjee [17,18] derived the equivalent symbolic expressions. Banerjee and Williams [19] later developed the explicit analytical expressions for the case of a Timoshenko beam and subsequently Banerjee et. al. [20] included the effects of warping.

This paper develops the exact dynamic stiffness matrix for a three-dimensional 'shear beam' with doubly asymmetric cross-section. Such a beam has the unusual theoretical property that it allows for both torsional and shearing deformation, but not bending deformation. The authors are unaware of any other work involving the vibration of shear beams, despite the fact that in the present case their use leads to a particularly simple member stiffness matrix that can be used very efficiently in the approximate determination of the lower natural frequencies of three-dimensional, multi-bay, multi-storey framed structures [21], including those that are doubly asymmetric on plan and which may contain step changes in member properties at one or more storey levels. However, a full description of the way in which the theory developed herein can be applied to such structures is beyond the scope of the current paper.

2. Theory

Fig. 1(a) shows a uniform, three-dimensional shear beam of length L, with doubly asymmetric cross-section. The origin of the coordinate system is located at the shear centre S, with the result that the elastic axis coincides with the z-axis. Point C on the cross-section denotes the centre of mass and its location in the coordinate system Sxy is given by x_c and y_c. The resulting mass axis

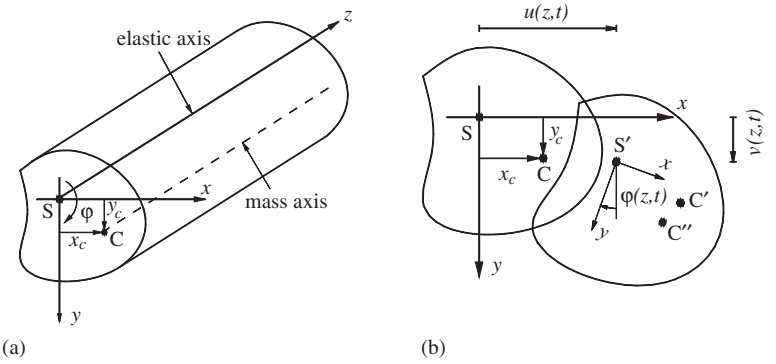

Fig. 1. (a) coordinate system and notation for a three-dimensional shear beam with doubly asymmetric cross-section, (b) typical displacement configuration of a cross-section.

then runs parallel to the z-axis through x_c, y_c. When the elastic axis and the mass axis of a beam do not coincide, the lateral and torsional motion of the beam will always be coupled in one or more planes.

During vibration, the displacement of the mass centre at any time t in the x–y plane can be determined as the result of a pure translation followed by a pure rotation about the shear centre, see Fig. 1. During the translation phase the shear centre S moves to S' and the mass centre C moves to C', displacements in each case of $u(z,t)$ and $v(z,t)$ in the x and y directions, respectively. During rotation, the mass centre moves additionally from C' to C'', an angular rotation of $\varphi(z,t)$ about S'. The resulting translation of the mass centre in the x–z and y–z planes, respectively, is

$$u(z,t) - y_c\varphi(z,t), \tag{1a}$$

$$v(z,t) + x_c\varphi(z,t). \tag{1b}$$

The coupled equations of motion that stem from the three orthogonal planes can now be developed from Figs. 1 and 2. In the x–z and y–z planes, this is achieved by equating the resultant shear force on the element to the corresponding product of mass and acceleration. In the x–y plane, the resultant torsional moment about the shear centre is equated to the sum of the moments

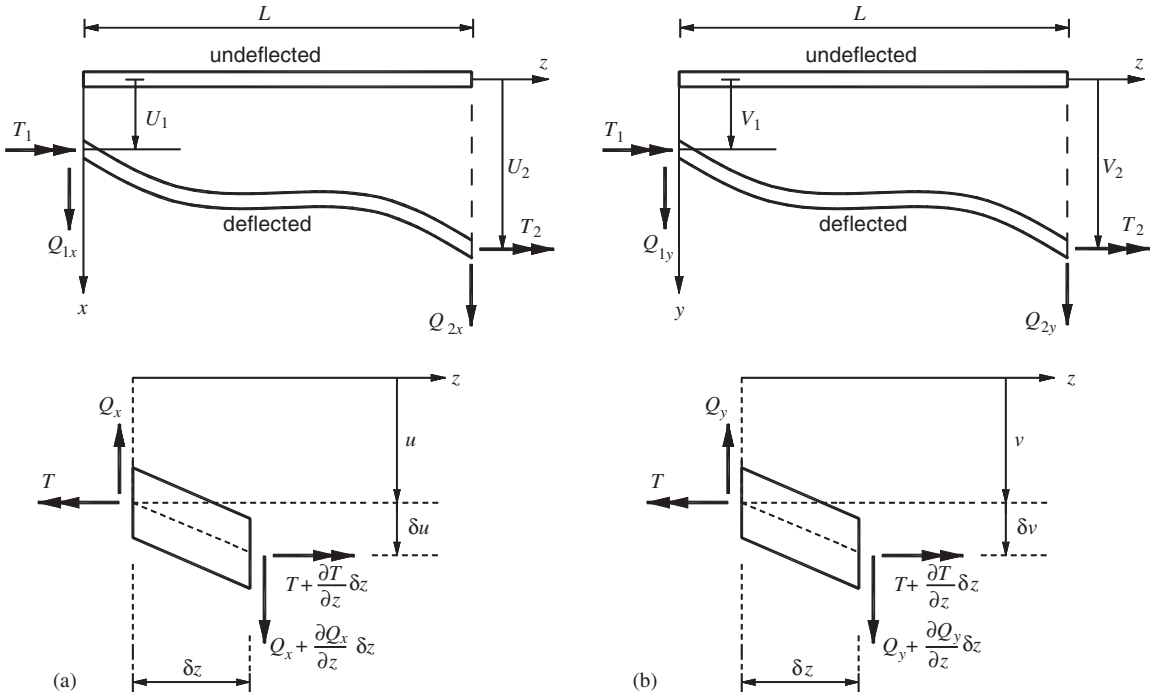

Fig. 2. End conditions for forces and displacements of a three-dimensional, doubly asymmetric shear beam (a) sign convention for force and displacement for the shear beam in the x–z plane (b) sign convention for force and displacement for the shear beam in the y–z plane.

of the mass accelerations about the same point. This yields

$$\frac{\partial Q_x(z,t)}{\partial z} = m\left(\frac{\partial^2 u(z,t)}{\partial t^2} - y_c\frac{\partial^2 \varphi(z,t)}{\partial t^2}\right), \tag{2a}$$

$$\frac{\partial Q_y(z,t)}{\partial z} = m\left(\frac{\partial^2 v(z,t)}{\partial t^2} + x_c\frac{\partial^2 \varphi(z,t)}{\partial t^2}\right), \tag{2b}$$

$$\frac{\partial T(z,t)}{\partial z} = m\left(r_m^2\frac{\partial^2 \varphi(z,t)}{\partial z^2} - y_c\frac{\partial^2 u(z,t)}{\partial t^2} + x_c\frac{\partial^2 v(z,t)}{\partial t^2}\right), \tag{2c}$$

where m is the mass/unit length of the member. The shear forces $Q_x(z,t)$, $Q_y(z,t)$ and the torsional moment $T(z,t)$ can be obtained from the appropriate stress/strain relationships as

$$Q_x(z,t) = GA_x\frac{\partial u(z,t)}{\partial z}, \tag{3a}$$

$$Q_y(z,t) = GA_y\frac{\partial v(z,t)}{\partial z}, \tag{3b}$$

$$T(z,t) = GJ\frac{\partial \varphi(z,t)}{\partial z} \tag{3c}$$

in which GA_x and GA_y are the effective shear rigidities of the beam in the x and y directions, respectively, GJ is the torsional rigidity of the cross-section and r_m is the polar mass radius of gyration of the cross-section about the z-axis.

Substituting Eqs. (3) into Eqs. (2) yields the required equations of motion as

$$GA_x\frac{\partial^2 u(z,t)}{\partial z^2} - m\frac{\partial^2 u(z,t)}{\partial t^2} + my_c\frac{\partial^2 \varphi(z,t)}{\partial t^2} = 0, \tag{4a}$$

$$GA_y\frac{\partial^2 v(z,t)}{\partial z^2} - m\frac{\partial^2 v(z,t)}{\partial t^2} - mx_c\frac{\partial^2 \varphi(z,t)}{\partial t^2} = 0, \tag{4b}$$

$$GJ\frac{\partial^2 \varphi(z,t)}{\partial z^2} + my_c\frac{\partial^2 u(z,t)}{\partial t^2} - mx_c\frac{\partial^2 v(z,t)}{\partial t^2} - mr_m^2\frac{\partial^2 \varphi(z,t)}{\partial z^2} = 0. \tag{4c}$$

Assuming harmonic motion, the instantaneous displacements can be written as

$$u(z,t) = U(z)\sin\omega t, \quad v(z,t) = V(z)\sin\omega t, \quad \varphi(z,t) = \Phi(z)\sin\omega t, \tag{5a–c}$$

where $U(z)$, $V(z)$ and $\Phi(z)$ are the amplitudes of the sinusoidally varying displacements.

Substituting Eqs. (5) into Eqs. (4) and re-writing in non-dimensional form gives

$$U''(\xi) + \omega^2\lambda_x^2 U(\xi) - y_c\omega^2\lambda_x^2\Phi(\xi) = 0, \tag{6a}$$

$$V''(\xi) + \omega^2\lambda_y^2 V(\xi) + x_c\omega^2\lambda_y^2\Phi(\xi) = 0, \tag{6b}$$

$$\Phi''(\xi) - \left(1/r_m^2\right)y_c\omega^2\lambda_\varphi^2 U(\xi) + \left(1/r_m^2\right)x_c\omega^2\lambda_\varphi^2 V(\xi) + \omega^2\lambda_\varphi^2\Phi(\xi) = 0, \tag{6c}$$

where

$$\lambda_x^2 = mL^2/GA_x, \quad \lambda_y^2 = mL^2/GA_y, \quad \lambda_\varphi^2 = r_m^2(mL^2/GJ) \text{ and } \xi = (z/L). \tag{7a–d}$$

Eqs. (6) can be re-written in the following matrix form:

$$\begin{bmatrix} D^2+\omega^2\lambda_x^2 & 0 & -y_c\omega^2\lambda_x^2 \\ 0 & D^2+\omega^2\lambda_y^2 & x_c\omega^2\lambda_y^2 \\ -(1/r_m^2)y_c\omega^2\lambda_\varphi^2 & (1/r_m^2)x_c\omega^2\lambda_\varphi^2 & D^2+\omega^2\lambda_\varphi^2 \end{bmatrix} \begin{bmatrix} U(\xi) \\ V(\xi) \\ \Phi(\xi) \end{bmatrix} = \mathbf{0} \tag{8}$$

in which $D = d/d\xi$.

Eq. (8) can be combined into one equation by eliminating either U, V or Φ to give the sixth-order differential equation

$$\begin{vmatrix} D^2+\omega^2\lambda_x^2 & 0 & -y_c\omega^2\lambda_x^2 \\ 0 & D^2+\omega^2\lambda_y^2 & x_c\omega^2\lambda_y^2 \\ -(1/r_m^2)y_c\omega^2\lambda_\varphi^2 & (1/r_m^2)x_c\omega^2\lambda_\varphi^2 & D^2+\omega^2\lambda_\varphi^2 \end{vmatrix} W(\xi) = 0, \tag{9}$$

where $W = U$, V or Φ.

The solution of Eq. (9) is found by substituting the trial solution $W(\xi) = e^{s\xi}$ to yield the characteristic equation

$$\begin{vmatrix} b^2+\lambda_x^2 & 0 & -y_c\lambda_x^2 \\ 0 & b^2+\lambda_y^2 & x_c\lambda_y^2 \\ -y_c\lambda_\varphi^2 & x_c\lambda_\varphi^2 & r_m^2(b^2+\lambda_\varphi^2) \end{vmatrix} = 0, \tag{10}$$

where $b^2 = (s/\omega)^2$.

Eq. (10) is a cubic equation in the frequency parameter b^2 and it can be proven (Appendix) that it always has three negative real roots. Let these three roots be $-b_1^2$, $-b_2^2$ and $-b_3^2$, where b_j^2 ($j = 1, 2, 3$) are all real and positive. Therefore

$$\left(\frac{s}{\omega}\right)^2 = -b_j^2 \quad \text{giving} \quad s = \pm \mathrm{i}\omega b_j \quad (j = 1, 2, 3) \quad \text{where } \mathrm{i} = \sqrt{-1}. \tag{11}$$

It follows that the solution of Eq. (9) can be written in the form

$$\begin{aligned} W(\xi) = {} & C_1 \cos b_1\omega\xi + C_2 \sin b_1\omega\xi + C_3 \cos b_2\omega\xi \\ & + C_4 \sin b_2\omega\xi + C_5 \cos b_3\omega\xi + C_6 \sin b_3\omega\xi. \end{aligned} \tag{12}$$

Eq. (12) represents the solution for $U(\xi)$, $V(\xi)$ and $\Phi(\xi)$, since they are all related via Eq. (8). They can be written individually as

$$\begin{aligned} U(\xi) = {} & t_1^u(C_1 \cos b_1\omega\xi + C_2 \sin b_1\omega\xi) + t_2^u(C_3 \cos b_2\omega\xi \\ & + C_4 \sin b_2\omega\xi) + t_3^u(C_5 \cos b_3\omega\xi + C_6 \sin b_3\omega\xi), \end{aligned} \tag{13a}$$

$$\begin{aligned} V(\xi) = {} & t_1^v(C_1 \cos b_1\omega\xi + C_2 \sin b_1\omega\xi) + t_2^v(C_3 \cos b_2\omega\xi \\ & + C_4 \sin b_2\omega\xi) + t_3^v(C_5 \cos b_3\omega\xi + C_6 \sin b_3\omega\xi), \end{aligned} \tag{13b}$$

$$\Phi(\xi) = C_1 \cos b_1\omega\xi + C_2 \sin b_1\omega\xi + C_3 \cos b_2\omega\xi + C_4 \sin b_2\omega\xi + C_5 \cos b_3\omega\xi + C_6 \sin b_3\omega\xi \tag{13c}$$

in which the constants t_j^u and t_j^v $(j = 1, 2, 3)$ are given by

$$t_j^u = \frac{y_c\lambda_x^2}{\lambda_x^2 - b_j^2} \quad (j = 1, 2, 3), \tag{14a}$$

$$t_j^v = \frac{-x_c\lambda_y^2}{\lambda_y^2 - b_j^2} \quad (j = 1, 2, 3). \tag{14b}$$

Substituting Eqs. (5) and (13) into Eq. (3) yields the equations for the lateral shear forces and torsional moment as

$$Q_x(z) = GA_x \frac{\mathrm{d}U(z)}{\mathrm{d}z} = \frac{1}{L} GA_x \frac{\mathrm{d}U(\xi)}{\mathrm{d}\xi}, \tag{15a}$$

$$Q_y(z) = GA_y \frac{\mathrm{d}V(z)}{\mathrm{d}z} = \frac{1}{L} GA_y \frac{\mathrm{d}V(\xi)}{\mathrm{d}\xi}, \tag{15b}$$

$$T(z) = GJ \frac{\mathrm{d}\Phi(z)}{\mathrm{d}z} = \frac{1}{L} GJ \frac{\mathrm{d}\Phi(\xi)}{\mathrm{d}\xi}. \tag{15c}$$

The nodal forces and displacements can now be defined in the member coordinate system of Figs. 2(a) and (b), as follows

$$\text{At } \xi = 0: \quad U = U_1, \quad V = V_1, \quad \Phi = \Phi_1, \quad Q_x = -Q_{1x}, \quad Q_y = -Q_{1y}, \quad T = -T_1, \tag{16a}$$

$$\text{At } \xi = 1: \quad U = U_2, \quad V = V_2, \quad \Phi = \Phi_2, \quad Q_x = Q_{2x}, \quad Q_y = Q_{2y}, \quad T = T_2. \tag{16b}$$

Then the nodal displacements can be determined from Eqs. (13) as

$$\begin{bmatrix} \mathbf{d}_1 \\ \mathbf{d}_2 \end{bmatrix} = \begin{bmatrix} \mathbf{E} & \mathbf{0} \\ \mathbf{0} & \mathbf{E} \end{bmatrix} \begin{bmatrix} \mathbf{I} & \mathbf{0} \\ \mathbf{C} & \mathbf{S} \end{bmatrix} \begin{bmatrix} \mathbf{C}_o \\ \mathbf{C}_e \end{bmatrix}, \tag{17}$$

where

$$\mathbf{d}_1 = \begin{bmatrix} U_1 \\ V_1 \\ \Phi_1 \end{bmatrix}, \quad \mathbf{d}_2 = \begin{bmatrix} U_2 \\ V_2 \\ \Phi_2 \end{bmatrix}, \quad \mathbf{C}_o = \begin{bmatrix} C_1 \\ C_3 \\ C_5 \end{bmatrix}, \quad \mathbf{C}_e = \begin{bmatrix} C_2 \\ C_4 \\ C_6 \end{bmatrix}, \quad \mathbf{E} = \begin{bmatrix} t_1^u & t_2^u & t_3^u \\ t_1^v & t_2^v & t_3^v \\ 1 & 1 & 1 \end{bmatrix},$$

$$\mathbf{C} = \begin{bmatrix} C_{b_1\omega} & 0 & 0 \\ 0 & C_{b_2\omega} & 0 \\ 0 & 0 & C_{b_3\omega} \end{bmatrix}, \quad \mathbf{S} = \begin{bmatrix} S_{b_1\omega} & 0 & 0 \\ 0 & S_{b_2\omega} & 0 \\ 0 & 0 & S_{b_3\omega} \end{bmatrix},$$

$$\mathbf{I} \text{ is the unit matrix}, \quad S_{b_j\omega} = \sin b_j\omega \text{ and } C_{b_j\omega} = \cos b_j\omega \quad (j = 1, 2, 3). \tag{18}$$

Hence the vector of constants $[\mathbf{C}_o\mathbf{C}_e]^{\mathrm{T}}$ can be determined from Eq. (17) as

$$\begin{bmatrix}\mathbf{C}_o\\ \mathbf{C}_e\end{bmatrix}=\begin{bmatrix}\mathbf{I} & \mathbf{0}\\ \mathbf{C} & \mathbf{S}\end{bmatrix}^{-1}\begin{bmatrix}\mathbf{E} & \mathbf{0}\\ \mathbf{0} & \mathbf{E}\end{bmatrix}^{-1}\begin{bmatrix}\mathbf{d}_1\\ \mathbf{d}_2\end{bmatrix}. \tag{19}$$

In similar fashion the vector of nodal forces can be determined from Eqs. (15) as

$$\begin{bmatrix}\mathbf{p}_1\\ \mathbf{p}_2\end{bmatrix}=\begin{bmatrix}\mathbf{DEb} & \mathbf{0}\\ \mathbf{0} & \mathbf{DEb}\end{bmatrix}\begin{bmatrix}\mathbf{0} & -\mathbf{I}\\ -\mathbf{S} & \mathbf{C}\end{bmatrix}\begin{bmatrix}\mathbf{C}_o\\ \mathbf{C}_e\end{bmatrix}, \tag{20}$$

where

$$\mathbf{p}_1=\begin{bmatrix}Q_{1x}\\ Q_{1y}\\ T_1\end{bmatrix},\quad \mathbf{p}_2=\begin{bmatrix}Q_{2x}\\ Q_{2y}\\ T_2\end{bmatrix},\quad \mathbf{D}=\frac{\omega}{L}\begin{bmatrix}GA_x & 0 & 0\\ 0 & GA_y & 0\\ 0 & 0 & GJ\end{bmatrix}\quad\text{and}\quad \mathbf{b}=\begin{bmatrix}b_1 & 0 & 0\\ 0 & b_2 & 0\\ 0 & 0 & b_3\end{bmatrix}. \tag{21}$$

Thus the required stiffness matrix can be developed by substituting Eq. (19) into Eq. (20) to give

$$\begin{bmatrix}\mathbf{p}_1\\ \mathbf{p}_2\end{bmatrix}=\begin{bmatrix}\mathbf{DEb} & \mathbf{0}\\ \mathbf{0} & \mathbf{DEb}\end{bmatrix}\begin{bmatrix}\mathbf{0} & -\mathbf{I}\\ -\mathbf{S} & \mathbf{C}\end{bmatrix}\begin{bmatrix}\mathbf{I} & \mathbf{0}\\ \mathbf{C} & \mathbf{S}\end{bmatrix}^{-1}\begin{bmatrix}\mathbf{E} & \mathbf{0}\\ \mathbf{0} & \mathbf{E}\end{bmatrix}^{-1}\begin{bmatrix}\mathbf{d}_1\\ \mathbf{d}_2\end{bmatrix} \tag{22}$$

or

$$\mathbf{p}=\mathbf{kd}. \tag{23}$$

The stiffness relationship of Eq. (23) is general and can be used in the normal way to assemble more complex forms. The required natural frequencies of the resulting structure are determined by evaluating its overall dynamic stiffness matrix at a trial frequency ω^* and using the Wittrick–Williams algorithm to establish how many natural frequencies have been exceeded by ω^*. This clearly provides the basis for a convergence procedure that can yield the required natural frequencies to any desired accuracy. The corresponding mode shapes can then be recovered by any appropriate method [8].

3. Wittrick–Williams algorithm

The dynamic structure stiffness matrix, $\mathbf{K}$, when assembled from the member stiffness matrices, yields the required natural frequencies as solutions of the equation

$$\mathbf{KD}=\mathbf{0}, \tag{24}$$

where $\mathbf{D}$ is the vector of amplitudes of the harmonically varying nodal displacements and $\mathbf{K}$ is a function of ω, the circular frequency. In most cases the required natural frequencies correspond to $|\mathbf{K}|$, the determinant of $\mathbf{K}$, being equal to zero. However, $\mathbf{K}$ is developed from exact member theory and the determinant is therefore a highly irregular, transcendental function of ω. Thus any trial and error method which involves computing $|\mathbf{K}|=0$ and noting when it changes sign through zero can miss roots. This can be overcome by use of the Wittrick–Williams algorithm [6,7] which has received wide attention in the literature [22]. The

algorithm states that

$$J = J_0 + s\{\mathbf{K}\}, \tag{25}$$

where J is the number of natural frequencies of the structure exceeded by some trial frequency, ω^*, J_0 is the number of natural frequencies that would still be exceeded if all members were clamped at their ends so as to make $\mathbf{D} = \mathbf{0}$ and s$\{\mathbf{K}\}$ is the sign count of the matrix $\mathbf{K}$. s$\{\mathbf{K}\}$ is defined in Ref. [7] and is equal to the number of negative elements on the leading diagonal of the upper triangular matrix obtained from $\mathbf{K}$, when $\omega = \omega^*$, by the standard form of Gauss elimination without row interchanges.

From the definition of J_0, it can be seen that

$$J_0 = \sum J_m, \tag{26}$$

where J_m is the number of natural frequencies of a member, with its end clamped, which have been exceeded by ω^*, and the summation extends over all members of the structure. In the present case it is possible to determine the value of J_m symbolically, using a direct approach, as follows.

The end conditions for a clamped–clamped member are

$$\mathbf{d}_1 = \mathbf{d}_2 = \mathbf{0}. \tag{27}$$

If Eq. (27) is substituted into Eq. (17) it is clear that the condition for non-trivial solutions is

$$\begin{vmatrix} \mathbf{E} & \mathbf{0} \\ \mathbf{0} & \mathbf{E} \end{vmatrix} \begin{vmatrix} \mathbf{I} & \mathbf{0} \\ \mathbf{C} & \mathbf{S} \end{vmatrix} = 0. \tag{28}$$

However, it is easy to show that the left-hand determinant can never be zero for a doubly asymmetric cross-section. Thus, noting that the right-hand determinant is that of a lower triangular matrix, Eq. (28) is only satisfied when the product of its significant leading diagonal terms is zero, i.e.

$$\prod_{j=1}^{3} S_{b_j\omega} = 0 \tag{29}$$

which is satisfied when

$$\omega_j^k = \frac{k\pi}{b_j}, \quad j = 1, 2, 3; \quad k = 1, 2, 3, \ldots \tag{30}$$

so J_m for any trial frequency ω^* can be found from

$$J_m = \text{int}\left[\frac{\omega^*}{(\pi/b_1)}\right] + \text{int}\left[\frac{\omega^*}{(\pi/b_2)}\right] + \text{int}\left[\frac{\omega^*}{(\pi/b_3)}\right] \tag{31}$$

in which int represents the image integer function, i.e. the greatest integer $< \omega^*/(\pi/b_j)$, $j = 1, 2, 3$.

4. Numerical results

Two examples are given in this section to clarify the foregoing theory. The first example demonstrates the application of the theory to the analysis of a stepped, three-dimensional shear beam with doubly asymmetric cross-section. The second example comprises a small parametric study that investigates the effects of eccentricity and the non-dimensional ratio $\lambda_y/\lambda_\varphi$ on the basic coupled natural frequencies of a shear cantilever with a singly asymmetric cross-section.

Example 1. A three-dimensional stepped shear beam with doubly asymmetric cross-section is now considered. The beam has both ends clamped and the properties of each of the stepped sections are given in Fig. 3. Young's modulus, E, for all sections is taken as $2\times10^{10}\,\mathrm{N/m^2}$. The eccentricities and polar mass radius of gyration of the cross-section about the z-axis for all sections in the coordinate system of Fig. 1 are $x_c = 0.2\,\mathrm{m}$, $y_c = 0.3\,\mathrm{m}$ and $r_m^2 = 0.23\,\mathrm{m^2}$.

The results for this example are given in Table 1. The second and third columns show the first 12 coupled and uncoupled natural frequencies of the beam obtained from the present theory, the latter being the frequencies calculated when $x_c \to y_c \to 0$. Table 2 validates the uncoupled frequencies for the structure of Example 1, by re-calculating them using the appropriate, exact dynamic stiffness matrix obtained from second-order theory corresponding to uncoupled motion in the x–y, x–z and y–z planes taken in turn. The results show exact agreement with the uncoupled natural frequencies obtained from the three-dimensional approach. However the authors are unaware of any published results or any other method that could reasonably be used to validate the results of the coupled natural frequencies.

Example 2. The second example comprises a small parametric study on a uniform cantilevered shear beam with singly asymmetric cross-section. It illustrates the effect on the natural frequencies of varying the eccentricity of the mass axis with respect to the elastic axis and the effect of varying the non-dimensional ratio $\lambda_y/\lambda_\varphi$, which is a measure of the relationship between the torsional and translational rigidities. The basic member properties are Young's modulus $= 2\times10^{10}\,\mathrm{N/m^2}$, length $= 6\,\mathrm{m}$, mass/unit length $= 5\times10^3\,\mathrm{kg/m}$, while the cross-section is symmetric about the x-axis ($y_c = 0$) and $r_{mc} = 0.1\,\mathrm{m}$, where r_{mc} is the polar mass radius of gyration of the cross-section about the mass centre.

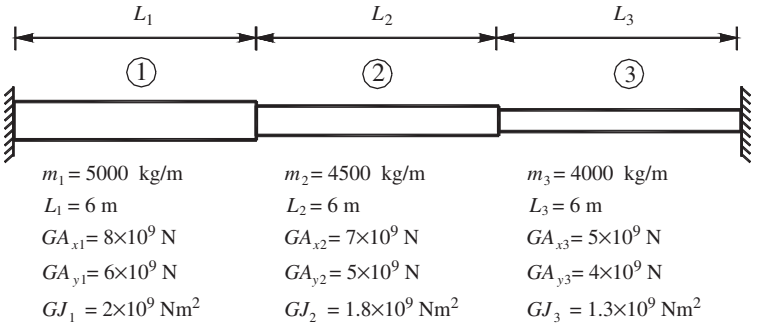

Fig. 3. Stepped shear beam with doubly asymmetric cross-section.

Table 1
The coupled and uncoupled natural frequencies of the beam of Example 1 using the present three-dimensional approach

Freq. no.	Coupled frequencies (Hz)	Uncoupled frequencies (Hz) ($x_c = y_c = 0$)
1	24.90	29.14
2	30.59	33.23
3	50.47	34.97
4	61.81	58.44
5	67.40	67.68
6	74.70	71.38
7	91.55	86.95
8	100.36	99.76
9	123.02	105.35
10	125.77	116.72
11	137.26	134.28
12	149.38	141.46

Table 2
The uncoupled natural frequencies of the beam of Example 1 using two-dimensional theory on each plane in turn

Freq. no.	x–z plane (Hz)	y–z plane (Hz)	x–y plane (Hz)
1	33.23	29.14	34.97
2	67.68	58.44	71.38
3	99.76	86.95	105.35
4	134.28	116.72	141.46

Three non-dimensional parameters are considered, namely the ratio $\lambda_y/\lambda_\varphi$, the coupling factor, f_c, and the eccentricity ratio e. Expressions for f_c and e are given as

$$f_c = \frac{\min(\omega_{1y}, \omega_{1\varphi})}{\omega_1}, \tag{32}$$

where ω_{1y} is the fundamental uncoupled frequency in the y–z plane, $\omega_{1\varphi}$ the fundamental uncoupled frequency in the x–y plane, ω_1 the fundamental coupled frequency and

$$e = x_c^2/r_m^2. \tag{33}$$

The coupling factor indicates the effect of eccentricity on the coupled fundamental frequency, while the eccentricity parameter represents a measure of the mass centre offset from the shear centre and is equal to zero in the case of two-fold symmetry. It is clear that e must lie in the range $0 \leqslant e \leqslant 1$, since $r_m^2 = r_{mc}^2 + x_c^2$, and the ratio $\lambda_y/\lambda_\varphi$ is assumed to vary from 0.2 to 5.

The graph of Fig. 4 shows the variation of f_c with $\lambda_y/\lambda_\varphi$ for a range of e values. It can be seen that maximum coupling occurs when $\lambda_y = \lambda_\varphi$. It also shows that the greater the mass centre offset, the greater the ratio of uncoupled to coupled natural frequencies becomes. Furthermore, it can be

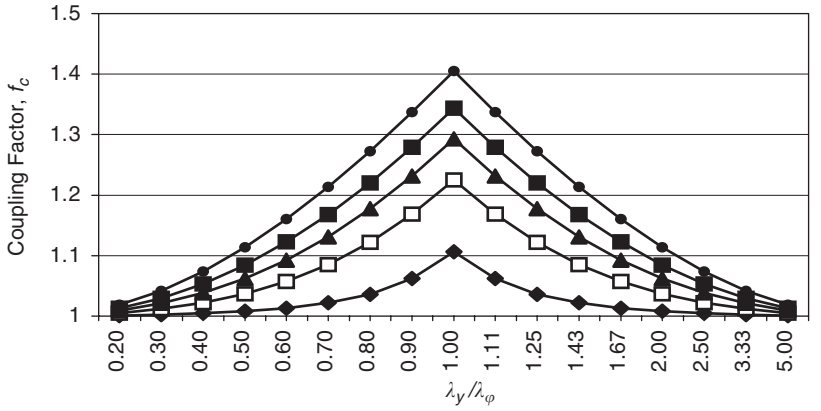

Fig. 4. Variation of the coupling factor f_c versus $\lambda_y/\lambda_\varphi$ for various values of e. $e = 0.05$, —◆—; $e = 0.25$, —□—; $e = 0.45$, —▲—; $e = 0.65$, —■—; $e = 0.95$, —•—.

concluded that the effect of coupling between modes is less than 10% when $e<0.05$ or $0.5<\lambda_y/\lambda_\varphi<2$ and may therefore be ignored to engineering accuracy.

5. Conclusions

An exact dynamic stiffness matrix has been developed for a three-dimensional shear beam with doubly asymmetric cross-section. The theory has been applied to the frequency analysis of a series of uniform shear cantilevers with singly asymmetric cross-sections. The results show that the most intense coupling of the modes occurs when the non-dimensional torsional and translational rigidities are equal. Guidance has been given as to when the effect of coupling can safely be ignored.

Appendix. The roots of Eq. (10)

For convenience Eq. (10) is re-written as a cubic function $f(\alpha)$ in which $\alpha = b^2$. This yields

$$f(\alpha) = \begin{vmatrix} \alpha + \lambda_x^2 & 0 & -y_c\lambda_x^2 \\ 0 & \alpha + \lambda_y^2 & x_c\lambda_y^2 \\ -y_c\lambda_\varphi^2 & x_c\lambda_\varphi^2 & r_m^2\left(\alpha + \lambda_\varphi^2\right) \end{vmatrix}. \tag{A.1}$$

The work of this appendix now proves that the three roots that make $f(\alpha) = 0$ are always negative real numbers. As a preliminary it should be noted that all the coefficients of Eq. (A.1) have real finite values. The typical cubic curve corresponding to $f(\alpha)$ is thus smooth and continuous and completely defined in the region of interest by the location of its roots and its value at $\alpha = 0$. See Fig. A.1(a).

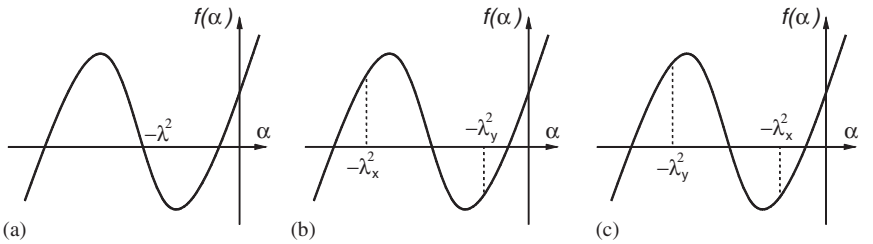

Fig. A.1. Diagram of $f(\alpha)$ versus α for the three cases of (a) $\lambda_x^2 = \lambda_y^2 = \lambda^2$ (b) $-\lambda_x^2 < -\lambda_y^2$ (c) $-\lambda_y^2 < -\lambda_x^2$.

From Eq. (A.1), $f(\alpha)$ may be written as

$$f(\alpha) = r_m^2(\alpha + \lambda_x^2)\left(\alpha + \lambda_y^2\right)\left(\alpha + \lambda_\varphi^2\right) - x_c^2\lambda_y^2\lambda_\varphi^2(\alpha + \lambda_x^2) - y_c^2\lambda_x^2\lambda_\varphi^2\left(\alpha + \lambda_y^2\right). \tag{A.2}$$

By inspection it can be seen that if $\lambda_x = \lambda_y = \lambda$, Eq. (A.2) becomes

$$f(\alpha) = (\alpha + \lambda^2)\left[r_m^2(\alpha + \lambda^2)\left(\alpha + \lambda_\varphi^2\right) - \lambda^2\lambda_\varphi^2\left(x_c^2 + y_c^2\right)\right] \tag{A.3}$$

and the roots may be calculated from

$$(\alpha + \lambda^2)\left[\alpha^2 + \beta\alpha + \gamma\right] = 0, \tag{A.4}$$

where

$$\beta = \lambda^2 + \lambda_\varphi^2 \text{ and } \gamma = \lambda^2\lambda_\varphi^2\left(r_m^2 - x_c^2 - y_c^2\right)/r_m^2. \tag{A.5}$$

The required roots $\alpha_j\,(j = 1, 2, 3)$ are therefore

$$\alpha_1 = -\lambda^2, \quad 2\alpha_2 = -\beta - \Delta \quad \text{and} \quad 2\alpha_3 = -\beta + \Delta, \tag{A.6}$$

where

$$\Delta^2 = \beta^2 - 4\gamma = \left(\lambda^2 - \lambda_\varphi^2\right)^2 + 4\lambda^2\lambda_\varphi^2\left(x_c^2 + y_c^2\right)/r_m^2 \tag{A.7}$$

α_1 is clearly a negative real root, as are α_2 and α_3, since

$$\Delta > 0, \quad \gamma > 0 \text{ and } -\beta < 0. \tag{A.8}$$

The more general result in which $\lambda_x^2 \neq \lambda_y^2$ can now be argued as follows. Consider the value of $f(0)$ that is obtained by substituting $\alpha = 0$ in Eq. (A.2). This gives

$$f(0) = \left(r_m^2 - x_c^2 - y_c^2\right)\lambda_x^2\lambda_y^2\lambda_\varphi^2 \tag{A.9}$$

in which r_m is the polar mass radius of gyration about the shear centre, S, and can be related to the polar mass radius of gyration about the centre of mass, r_{mc}, through the following equation:

$$r_m^2 = r_{mc}^2 + x_c^2 + y_c^2 \tag{A.10}$$

therefore

$$f(0) = r_{mc}^2 \lambda_x^2 \lambda_y^2 \lambda_\varphi^2 \tag{A.11}$$

which is the product of four positive parameters and therefore $f(0)$ is always positive with a limiting (trivial) value of zero. It is equally easy to show that

$$f(\infty) = \infty \quad \text{and} \quad f(-\infty) = -\infty. \tag{A.12}$$

In similar fashion, substituting the values of $\alpha = -\lambda_x^2$ and $\alpha = -\lambda_y^2$ into Eq. (A.2) yields

$$f\left(-\lambda_x^2\right) = -y_c^2 \lambda_x^2 \lambda_\varphi^2 \left(\lambda_y^2 - \lambda_x^2\right) \tag{A.13}$$

and

$$f\left(-\lambda_y^2\right) = -x_c^2 \lambda_y^2 \lambda_\varphi^2 \left(\lambda_x^2 - \lambda_y^2\right). \tag{A.14}$$

We now wish to consider the two cases in which $-\lambda_x^2 < -\lambda_y^2$ and $-\lambda_y^2 < -\lambda_x^2$ and note that $\lambda_x^2 = \lambda_y^2$ corresponds to the case originally discussed.

Thus, when $-\lambda_x^2 < -\lambda_y^2$, Eqs. (A.11)–(A.14) give

$$f(0) > 0, \quad f\left(-\lambda_y^2\right) < 0, \quad f\left(-\lambda_x^2\right) > 0 \quad \text{and} \quad f(-\infty) < 0. \tag{A.15}$$

These imply that there are three negative real roots of the function $f(\alpha)$ in the intervals $(0, -\lambda_y^2)$, $(-\lambda_y^2, -\lambda_x^2)$ and $(-\lambda_x^2, -\infty)$. See Fig. A.1(b).

Similarly, when $-\lambda_y^2 < -\lambda_x^2$, Eqs. (A.11)–(A.14) give

$$f(0) > 0, \quad f\left(-\lambda_x^2\right) < 0, \quad f\left(-\lambda_y^2\right) > 0 \quad \text{and} \quad f(-\infty) < 0 \tag{A.16}$$

which again imply that there are three negative real roots of the function $f(\alpha)$ in the intervals $(0, -\lambda_x^2)$, $(-\lambda_x^2, -\lambda_y^2)$ and $(-\lambda_y^2, -\infty)$. See Fig. A.1(c).

References

[1] S. Blaszkowiak, Z. Kaczkowski, *Iterative Methods in Structural Analysis*, Pergamon Press, Oxford, 1966.
[2] M.E. Mohsin, E.A. Sadek, The distributed mass-stiffness technique for the dynamical analysis of complex frameworks, *The Structural Engineer* 46 (1968) 345–351.
[3] R.D. Henshell, G.B. Warburton, Transmission of vibration in beam systems, *International Journal for Numerical Methods in Engineering* 1 (1969) 47–66.
[4] F.Y. Cheng, Vibrations of Timoshenko beams and frameworks, *Journal of Structural Engineering* 96 (ST3) (1970) 551–571.
[5] T.M. Wang, T.A. Kinsman, Vibration of frame structures according to the Timoshenko theory, *Journal of Sound and Vibration* 14 (1971) 215–227.
[6] F.W. Williams, W.H. Wittrick, An automatic computational procedure for calculating natural frequencies of skeletal structures, *International Journal of Mechanical Sciences* 12 (1970) 781–791.
[7] W.H. Wittrick, F.W. Williams, A general algorithm for computing natural frequencies of elastic structures, *The Quarterly Journal of Mechanics and Applied Mathematics* 24 (3) (1971) 263–284.

[8] W.P. Howson, A compact method for computing the eigenvalues and eigenvectors of plane frames, *Advances in Engineering Software and Workstations* 1 (4) (1979) 181–190.
[9] W.P. Howson, J.R. Banerjee, F.W. Williams, Concise equations and program for exact eigensolutions of plane frames including member shear, *Advances in Engineering Software and Workstations* 5 (3) (1983) 137–141.
[10] W.P. Howson, F.W. Williams, Natural frequencies of frames with axially loaded Timoshenko members, *Journal of Sound and Vibration* 26 (4) (1973) 503–515.
[11] W.P. Howson, A.K. Jemah, Exact dynamic stiffness method for planar natural frequencies of curved Timoshenko beams, *Proceedings of the Institution of Mechanical Engineers Part C— Journal of Mechanical Engineering Science* 213 (7) (1999) 687–696.
[12] W.P. Howson, A.K. Jemah, Exact out-of-plane natural frequencies of curved Timoshenko beams, *Journal of Engineering Mechanics* 125 (1) (1999) 19–25.
[13] F.W. Williams, W.P. Howson, J.R. Banerjee, Natural frequencies of members with coupled extensional–torsional motion—a physical approach, *Journal of Sound and Vibration* 165 (2) (1993) 373–375.
[14] W.L. Hallauer, Y.L. Liu, Beam bending-torsion dynamic stiffness method for calculation of exact vibration modes, *Journal of Sound and Vibration* 85 (1) (1982) 105–113.
[15] P.O. Friberg, Coupled vibrations of beams—an exact dynamic element stiffness matrix, *International Journal for Numerical Methods in Engineering* 19 (4) (1983) 479–493.
[16] P.O. Friberg, Beam element matrices derived from Vlasovs theory of open thin-walled elastic beams, *International Journal for Numerical Methods in Engineering* 21 (7) (1985) 1205–1228.
[17] J.R. Banerjee, Coupled bending torsional dynamic stiffness matrix for beam elements, *International Journal for Numerical Methods in Engineering* 28 (6) (1989) 1283–1298.
[18] J.R. Banerjee, A Fortran routine for computation of coupled bending–torsional dynamic stiffness matrix of beam elements, *Advances in Engineering Software and Workstations* 13 (1) (1991) 17–24.
[19] J.R. Banerjee, F.W. Williams, Coupled bending–torsional dynamic stiffness matrix for Timoshenko beam elements, *Computers & Structures* 42 (3) (1992) 301–310.
[20] J.R. Banerjee, S. Guo, W.P. Howson, Exact dynamic stiffness matrix of a bending-torsion coupled beam including warping, *Computers & Structures* 59 (4) (1996) 613–621.
[21] B. Rafezy, W.P. Howson. Natural frequencies of plane sway frames: an overview of two simple models, in: *Proceedings of the International Conference on Computational and Experimental Engineering and Sciences (ICCES'03)*, Corfu, Greece, Paper 339, 2003, p6.
[22] F.W. Williams, W.H. Wittrick, Exact buckling and frequency calculations surveyed, *Journal of Structural Engineering* 109 (1) (1983) 169–187.